A benchmark of a single-surface yield function with hardening - Ehlers material model

Xing-Yuan Miao

A seven-parametric yield function presented by Ehlers (1995) is expressed as:

$$F = \Phi^{\frac{1}{2}} + \beta I_1 + \varepsilon I_1^2 - k(\varepsilon_{\mathrm{p\,eff}}) \tag{1}$$

$$\Phi = J_2\left(1+\gamma\vartheta\right)^m + \frac{1}{2}\alpha I_1^2 + \delta^2 I_1^4 \tag{2}$$

$$\vartheta = \frac{J_3}{J_2^{\frac{3}{2}}} \tag{3}$$

For general statement, the plastic potential is considered as:

$$G_F = F \tag{4}$$

The derivation of the plastic flow rule and the partial linearisation proceed as follows:

$$\frac{\partial G_F}{\partial \boldsymbol{\sigma}} = \frac{1}{2\Phi^{\frac{1}{2}}}\frac{\partial \Phi}{\partial \boldsymbol{\sigma}} + \beta\frac{\partial I_1}{\partial \boldsymbol{\sigma}} + 2\varepsilon I_1\frac{\partial I_1}{\partial \boldsymbol{\sigma}} \tag{5}$$

$$= \frac{1}{2\Phi^{\frac{1}{2}}}\frac{\partial \Phi}{\partial \boldsymbol{\sigma}} + \beta\mathbf{I} + 2\varepsilon I_1\mathbf{I} \tag{6}$$

$$\frac{\partial \Phi}{\partial \boldsymbol{\sigma}} = \left(1+\gamma\vartheta\right)^m\frac{\partial J_2}{\partial \boldsymbol{\sigma}} + m\gamma J_2\left(1+\gamma\vartheta\right)^{m-1}\frac{\partial \vartheta}{\partial \boldsymbol{\sigma}} + \alpha I_1\frac{\partial I_1}{\partial \boldsymbol{\sigma}} + 4\delta^2 I_1^3\frac{\partial I_1}{\partial \boldsymbol{\sigma}} \tag{7}$$

$$= \left(1+\gamma\vartheta\right)^m\boldsymbol{\sigma}^{\mathrm{D}} + m\gamma J_2\left(1+\gamma\vartheta\right)^{m-1}\frac{\partial \vartheta}{\partial \boldsymbol{\sigma}} + \alpha I_1\mathbf{I} + 4\delta^2 I_1^3\mathbf{I} \tag{8}$$

where

$$\frac{\partial \vartheta}{\partial \boldsymbol{\sigma}} = \frac{\partial \vartheta}{\partial J_3}\frac{\partial J_3}{\partial \boldsymbol{\sigma}} + \frac{\partial \vartheta}{\partial J_2}\frac{\partial J_2}{\partial \boldsymbol{\sigma}} = \frac{1}{J_2^{\frac{3}{2}}}\frac{\partial J_3}{\partial \boldsymbol{\sigma}} - \frac{3}{2}\frac{J_3}{J_2^{\frac{5}{2}}}\frac{\partial J_2}{\partial \boldsymbol{\sigma}} = \vartheta\left(\boldsymbol{\sigma}^{\mathrm{D}-1}\right)^{\mathrm{D}} - \frac{3}{2}\frac{\vartheta}{J_2}\boldsymbol{\sigma}^{\mathrm{D}} \tag{9}$$

$$\frac{\partial J_3}{\partial \boldsymbol{\sigma}} = J_3\left(\boldsymbol{\sigma}^{\mathrm{D}-1}\right)^{\mathrm{D}} \tag{10}$$

$$\frac{\partial J_2}{\partial \boldsymbol{\sigma}} = \boldsymbol{\sigma}^{\mathrm{D}} \tag{11}$$

$$\frac{\partial I_1}{\partial \boldsymbol{\sigma}} = \mathbf{I} \tag{12}$$

$$\frac{\partial \boldsymbol{\sigma}^{\mathrm{D}}}{\partial \boldsymbol{\sigma}} = \mathscr{P}^{\mathrm{D}} \tag{13}$$

so that

$$\boldsymbol{f}^{\mathrm{D}} = \frac{1}{2\Phi^{\frac{1}{2}}}\left(\left(\left(1+\gamma\vartheta\right)^m\right)\boldsymbol{\sigma}^{\mathrm{D}} + m\gamma J_2\left(1+\gamma\vartheta\right)^{m-1}\frac{\partial \vartheta}{\partial \boldsymbol{\sigma}}\right. \tag{14}$$

$$\boldsymbol{f}^{\mathrm{S}} = \frac{1}{2\Phi^{\frac{1}{2}}}\left(\alpha I_1 + 4\delta^2 I_1^3\right)\mathbf{I} + \left(\beta + 2\varepsilon I_1\right)\mathbf{I} \tag{15}$$

$$f^{\mathrm{S}} = \frac{3}{2\Phi^{\frac{1}{2}}}\left(\alpha I_1 + 4\delta^2 I_1^3\right) + 3\left(\beta + 2\varepsilon I_1\right) \tag{16}$$

Thus, the non-zero Jacobian's component relations are:

$$\frac{\partial F}{\partial \tilde{\sigma}^j} = G\left[\frac{\partial F}{\partial I_1}\mathbf{I} + \left(\frac{\partial F}{\partial J_2} + \frac{\partial F}{\partial \vartheta}\frac{\partial \vartheta}{\partial J_2}\right)\boldsymbol{\sigma}^{\mathrm{D}} + \frac{\partial F}{\partial \vartheta}\frac{\partial \vartheta}{\partial J_3}J_3\boldsymbol{\sigma}^{\mathrm{D}-1} : \mathscr{P}^{\mathrm{D}}\right] \tag{17}$$

$$\frac{\partial \boldsymbol{f}^{\mathrm{S}}}{\partial \tilde{\sigma}^j} = G\left[-\frac{3}{4\Phi^{\frac{3}{2}}}\left(\alpha I_1 + 4\delta^2 I_1^3\right)\frac{\partial \Phi}{\partial \boldsymbol{\sigma}} + \frac{3}{2\Phi^{\frac{1}{2}}}\left(\alpha + 12\delta^2 I_1^2\right)\mathbf{I} + 6\varepsilon\mathbf{I}\right] \tag{18}$$

$$\frac{\partial \boldsymbol{f}^{\mathrm{D}}}{\partial \tilde{\sigma}^j} = G\left[-\frac{1}{4\Phi^{\frac{3}{2}}}\boldsymbol{M}_1 + \frac{1}{2\Phi^{\frac{1}{2}}}\left(\boldsymbol{M}_2 + \boldsymbol{M}_3\right)\right] \tag{19}$$

where

$$\frac{\partial \boldsymbol{\sigma}^j}{\partial \tilde{\boldsymbol{\sigma}}^j} = G \tag{20}$$

$$\boldsymbol{M}_1 = (1+\gamma\vartheta)^m\,\boldsymbol{\sigma}^{\mathrm{D}} \otimes \frac{\partial \Phi}{\partial \boldsymbol{\sigma}} + m\gamma J_2\,(1+\gamma\vartheta)^{m-1}\,\frac{\partial \vartheta}{\partial \boldsymbol{\sigma}} \otimes \frac{\partial \Phi}{\partial \boldsymbol{\sigma}} \tag{21}$$

$$\boldsymbol{M}_2 = (1+\gamma\vartheta)^m\,\mathscr{P}^{\mathrm{D}} + m\gamma\,(1+\gamma\vartheta)^{m-1}\,\frac{\partial \vartheta}{\partial \boldsymbol{\sigma}} \otimes \boldsymbol{\sigma}^{\mathrm{D}} \tag{22}$$

$$\boldsymbol{M}_3 = m\gamma\left((1+\gamma\vartheta)^{m-1}\,\boldsymbol{\sigma}^{\mathrm{D}} \otimes \frac{\partial \vartheta}{\boldsymbol{\sigma}} + J_2(m-1)\gamma\,(1+\gamma\vartheta)^{m-2}\,\frac{\partial \vartheta}{\boldsymbol{\sigma}} \otimes \frac{\partial \vartheta}{\boldsymbol{\sigma}} + J_2\,(1+\gamma\vartheta)^{m-1}\,\frac{\partial^2 \vartheta}{\partial \boldsymbol{\sigma}^2}\right) \tag{23}$$

$$\frac{\partial^2 \vartheta}{(\partial \boldsymbol{\sigma})^2} = \left(\boldsymbol{\sigma}^{\mathrm{D}-1}\right)^{\mathrm{D}} \otimes \frac{\partial \vartheta}{\partial \boldsymbol{\sigma}} - \vartheta\mathscr{P}^{\mathrm{D}} : \left(\boldsymbol{\sigma}^{\mathrm{D}-1} \odot \boldsymbol{\sigma}^{\mathrm{D}-1}\right) : \mathscr{P}^{\mathrm{D}} - \frac{3}{2}\left(\frac{1}{J_2}\boldsymbol{\sigma}^{\mathrm{D}} \otimes \frac{\partial \vartheta}{\partial \boldsymbol{\sigma}} + \frac{\vartheta}{J_2}\mathscr{P}^{\mathrm{D}} - \frac{\vartheta}{J_2^2}\boldsymbol{\sigma}^{\mathrm{D}} \otimes \boldsymbol{\sigma}^{\mathrm{D}}\right) \tag{24}$$

The 15×15 Jacobian reads:

$$\frac{\partial \boldsymbol{G}}{\partial z} = \begin{pmatrix} \boldsymbol{J}_{11} & \boldsymbol{J}_{12} & \boldsymbol{J}_{13} & \boldsymbol{J}_{14} & \boldsymbol{J}_{15} \\ \boldsymbol{J}_{21} & \boldsymbol{J}_{22} & \boldsymbol{J}_{23} & \boldsymbol{J}_{24} & \boldsymbol{J}_{25} \\ \boldsymbol{J}_{31} & \boldsymbol{J}_{32} & J_{33} & J_{34} & J_{35} \\ \boldsymbol{J}_{41} & \boldsymbol{J}_{42} & J_{43} & J_{44} & J_{45} \\ \boldsymbol{J}_{51} & \boldsymbol{J}_{52} & J_{53} & J_{54} & J_{55} \end{pmatrix} \tag{25}$$

where the components are given as follows:

$$\boldsymbol{J}_{11} = \boldsymbol{I}, \quad \boldsymbol{J}_{12} = 2\boldsymbol{I}, \quad \boldsymbol{J}_{13} = \frac{K}{G}\boldsymbol{I}, \quad \boldsymbol{J}_{14} = \boldsymbol{J}_{15} = \boldsymbol{0} \tag{26}$$

$$\boldsymbol{J}_{21} = -\lambda^j\frac{\partial \boldsymbol{f}^{\mathrm{D}}}{\partial \tilde{\sigma}^j}, \quad \boldsymbol{J}_{22} = \frac{1}{\Delta t}\boldsymbol{I}, \quad \boldsymbol{J}_{23} = \boldsymbol{J}_{24} = \boldsymbol{0}, \quad \boldsymbol{J}_{25} = -\boldsymbol{f}^{\mathrm{D}} \tag{27}$$

$$\boldsymbol{J}_{31} = -\lambda^j\frac{\partial f^{\mathrm{S}}}{\partial \tilde{\sigma}^j}, \quad \boldsymbol{J}_{32} = \boldsymbol{0}, \quad J_{33} = \frac{1}{\Delta t}, \quad J_{34} = 0, \quad J_{35} = -f^{\mathrm{S}} \tag{28}$$

$$\boldsymbol{J}_{41} = -\frac{2\left(\lambda^j\right)^2}{3\sqrt{\frac{2}{3}\left(\lambda^j\right)^2\boldsymbol{f}^{\mathrm{D}}\cdot\boldsymbol{f}^{\mathrm{D}}}}\frac{\partial \boldsymbol{f}^{\mathrm{D}}}{\partial \tilde{\sigma}^j}\boldsymbol{f}^{\mathrm{D}}, \quad \boldsymbol{J}_{42} = \boldsymbol{0}, \quad J_{43} = 0, \quad J_{44} = \frac{1}{\Delta t}, \quad J_{45} = -\frac{2\lambda^j\boldsymbol{f}^{\mathrm{D}}\cdot\boldsymbol{f}^{\mathrm{D}}}{3\sqrt{\frac{2}{3}\left(\lambda^j\right)^2\boldsymbol{f}^{\mathrm{D}}\cdot\boldsymbol{f}^{\mathrm{D}}}} \tag{29}$$

$$\boldsymbol{J}_{51} = \frac{\partial F}{\partial \tilde{\sigma}^j}, \quad \boldsymbol{J}_{52} = \boldsymbol{0}, \quad J_{53} = 0, \quad J_{54} = -\frac{\kappa h}{G}, \quad J_{55} = 0 \tag{30}$$

$$\tag{31}$$

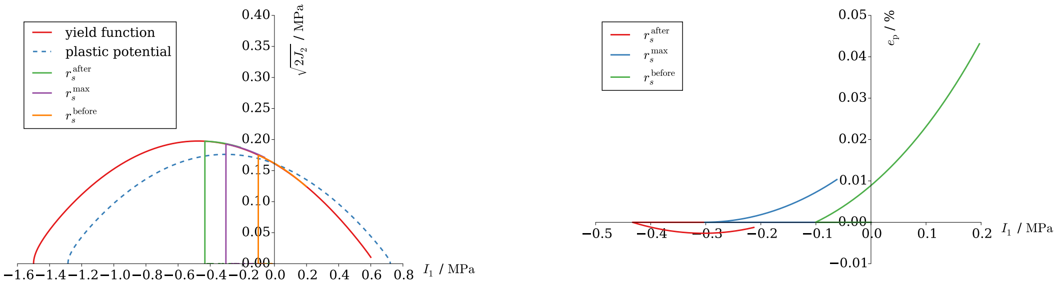

Figure 1: Characteristic shape of the yield function and the plastic potential in the hydrostatic plane and the corresponding plastic volumetric strain when I_1 = const., α = 0.

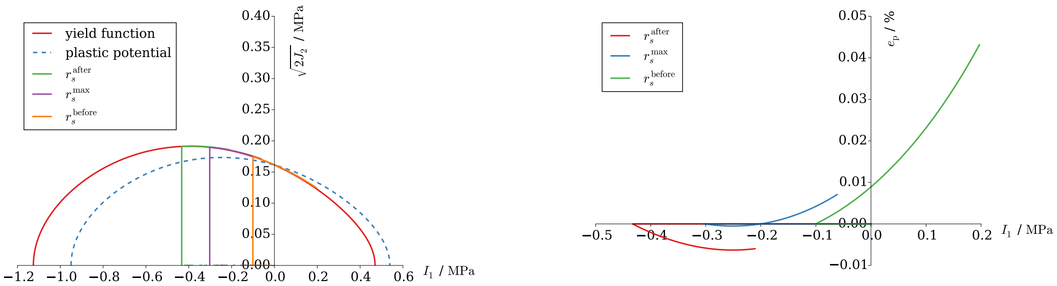

Figure 2: Characteristic shape of the yield function and the plastic potential in the hydrostatic plane and the corresponding plastic volumetric strain when I_1 = const., α = 0.01.

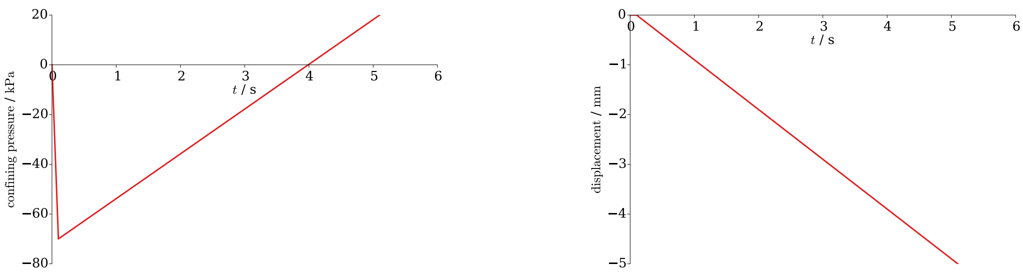

Figure 3: Triaxial compression test.

The specific material under case study refers to the one that used in the work of Ehlers and Avci (2013).

Table 1: Values of the parameters describing elastic process and plastic hardening

Shear modulus G MN/mm^2	Bulk modulus K MN/mm^2	Hardening h	κ mm^2/MN	β	γ	α	δ mm^2/MN	ϵ mm^2/MN	m
150	200	10	0.1	0.095	1	0.01	0.0078	0.1	0.54
				β_p	γ_p	α_p	δ_p	ϵ_p	m_p
				0.0608	1	0.01	0.0078	0.1	0.54

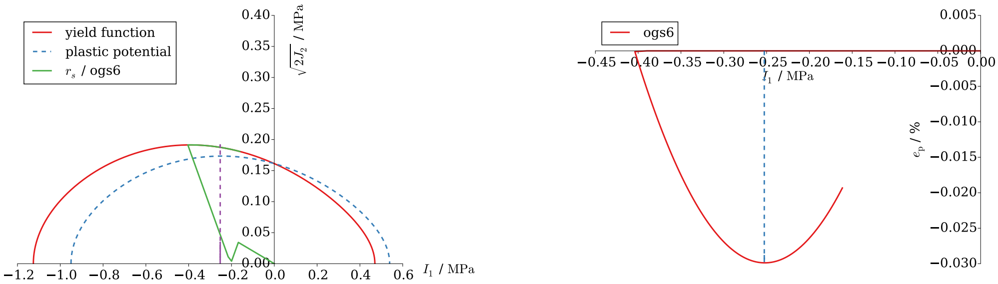

Figure 4: Variations of the stress states and the plastic volumetric strain with monotonic loading process.

The parameter set is listed in Table 1. A conventional triaxial compression test was performed under the condition of i) I_1 = const.; ii) I_1 monotonically increases with time, see Fig. 3 in loading process and confining pressure $\sigma_1 = \sigma_2 = \sigma_3 = \frac{1}{3}I_1$. During the compression test, a continuous displacement-controlled loading process was applied with a velocity of 1 mm/s. For the yield function in the hydrostatic plane, the consolidation pressure p_c and the ratio π_c which defines the ratio between the pressures corresponding to the curve's maximum and length can be expressed as functions of β, δ and ϵ:

$$p_c = \frac{\beta}{3\,(\epsilon + \delta)} \tag{32}$$

$$\pi_c = \frac{1}{4\,(\epsilon - \delta)}\left(3\epsilon - \sqrt{8\delta^2 + \epsilon^2}\right) \tag{33}$$

Note that, only in the case of $\alpha = 0$, the curve's maximum depends on p_c and π_c, see Fig. 1 and Fig. 2 for comparison.

Fig. 4 shows a triaxial compression test under a monotonic confining pressure. The volume deformation varies rapidly from a slight contraction to a significant dilatation behaviour during the specific loading path. The plastic volumetric strain exhibits a nonlinear progression over the loading process. Two states are worth noted, i) the effective shear stress vanishes at a constant stage under the current ongoing confining pressure and displacement loading; ii) The plastic volumetric strain achieves the maximum, and then, the declining stage illustrates the decrease of the volume dilatation.

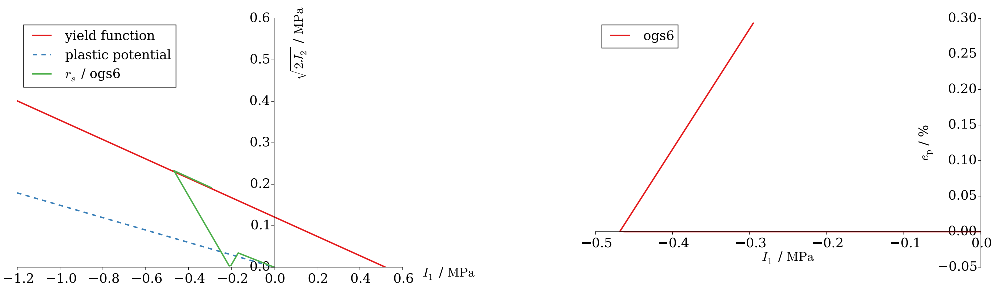

Figure 5: Variations of the stress states and the plastic volumetric strain with monotonic loading process (Drucker-Prager yield criterion).

By prescribing specific parameters to be zero, the seven-parametric yield function can be reduced to the well-known criteria, such as the Drucker-Prager and von Mises. Here, we provide a Drucker-Prager model test as an additional verification of the Ehlers material model, see Fig. 5. Note that, the reduction of the Ehlers material model corresponds to the state that the Drucker–Prager yield surface middle circumscribes the Mohr–Coulomb yield surface.

References

Ehlers, W., 1995. A single-surface yield function for geomaterials. Archive of Applied Mechanics 65 (4), 246–259.

Ehlers, W., Avci, O., 2013. Stress-dependent hardening and failure surfaces of dry sand. International Journal for Numerical and Analytical Methods in Geomechanics 37 (8), 787–809.